Improved Quasi-TEM Spectral Domain Analysis Of Boxed Coplanar Multiconductor Microstrip Lines

Enrique Drake, Francisco Medina, *Member, IEEE,* and Manuel Horno, *Member, IEEE*

Abstract— **This paper presents a very efficient quasi-TEM analysis of multistrip transmission systems embedded in a layered medium. The number of conductors and substrates is arbitrary, and the whole structure is assumed to be enclosed in a rectangular set of boundary conditions. The analysis makes use of the Galerkin method in the spectral domain. Chebyshev polynomials with edge conditions are used as basis and test functions for the strips free charge distribution. This standard technique is considerably enhanced by means of two alternative procedures to accelerate the computation of the entries of the Galerkin matrix. Extremely accurate results for a multistrip system, including the charge distribution, can then be obtained on a PC computer in a short CPU time.**

I. Introduction

MULTICONDUCTOR TRANSMISSION LINES (MTL) are widely used in (monolithic) microwave integrated circuits, high speed interconnecting buses and other applications. Once the propagation characteristics of a MTL system are known, its frequency domain or time domain electrical responses can be obtained by means of well known methods. The propagation parameters have been computed by means of both quasi-TEM and full-wave approaches. In many practical situations the quasi-TEM analysis provides results which are accurate enough, and in these cases it is prefered to the much more computationally involved full-wave approach. In addition, quasi-TEM data can be used as an initial guess in full-wave algorithms, thus improving their efficiency.

If quasi-TEM operation is assumed, the propagation parameters are computed from the capacitance, $[C]$, and inductance, $[L]$, per unit length (p.u.l.) matrices of the MTL. Powerful methods have been reported in the literature to compute $[C]$ and $[L]$ for multiconductor systems having arbitrary geometry [1]–[3] or planar geometry [4], [5]. Specific techniques have also been developed for microstrip geometries, which result in particularly efficient computer algorithms. For instance, some multiconductor structures can be exactly solved by using conformal mapping [6], [7] or very efficiently handled by means of the integral equation technique [8]. For the general microstrip-like geometry embedded in a layered linear medium (see Fig.1) the spectral domain approach (SDA) - combined with the Galerkin method [9, 10], variational formulation [11], [12] or iterative techniques [13], [14] - is probably the most simple and widely used tool. Although the direct application of these techniques gives place to accurate, reliable and quick computer codes, proper analytical preprocessing drastically improves their performance. A variety of techniques involving heavy analytical work has been applied to the solution of the single microstrip problem (see [15] and the references therein).

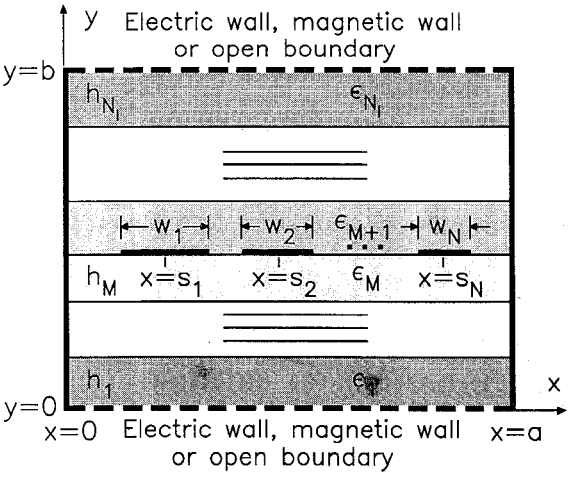

Fig. 1. Cross section of the generalized boxed coplanar multistrip line under study.

The present paper is a meaningful extension of the work in [15] which deals with multistrip geometries having arbitrary strip widths. The technique is essentially an enhanced spectral domain analysis. Two efficient schemes are provided to accelerate the computation of the spectral series involved in the Galerkin matrix in a drastical way. The application of these techniques makes it possible to compute the characteristic parameters of the microstrip MTL in Fig. 1 with high accuracy in a short CPU time. The charge distribution is simultaneously obtained with extreme accuracy. The analysis of a typical multistrip system can be carried out on a PC/AT computer with math coprocessor in no more than one or two seconds. The developed programs can be used for CAD applications on a workstation. This software could be useful for engineers dealing with multistrip geometries.

II. Statement of the Problem

The cross section of the microstrip-like system considered in this work is shown in Fig. 1. Translational symmetry in the z direction is assumed. An arbitrary number, N, of zero-thickness perfectly conducting strips are placed on the Mth interface of a N_l-layered medium. The ith strip is

Manuscript received February 24, 1992; revised May 26, 1992. This work was supported by the DGICYT, Spain (Project No. TIC91-1018).

The authors are with the Departamento de Electronica y Electromagnetismo, Facultad de Física, Universidad de Sevilla, Avda. Reina Mercedes s/n, 41012 Sevilla, Spain.

IEEE Log Number 9204482.

characterized by its width, w_i, and the position, s_i, of its middle point. The layered substrate is composed of N_l slabs of lossless/lossy/iso/anisotropic linear materials. The jth layer is characterized by its complex dielectric permittivity tensor, $\hat{\epsilon}_j$, (or equivalent permittivity tensor [10]). The structure is enclosed into a rectangular frame bounded by the planes $x = 0, x = a, y = 0, y = b$ (see Fig. 1). A wide family of coplanar microstrip-like transmission lines can be considered to be a particular case of this generic structure.

As it is well known, all the quasi-TEM parameters of the MTL system can be obtained from its capacitance, $[C]$, and inductance, $[L]$, p.u.l. matrices. Usually $[L]$ is computed from the capacitance p.u.l. matrix, $[C']$, of a proper related structure [10]. Then, the quasi-TEM analysis reduces to solving two electrostatic-type bidimensional problems. Each coefficient C_{ij} $(i, j = 1, \ldots, N)$ of $[C]$ or $[C']$ can be defined as the free charge on the ith strip when the jth strip is set to voltage unity and the rest of the strips are grounded (canonical excitation). Therefore the computation of $[C]$ (or $[C']$) requires to solve the free charge density integral equation N times (for N canonical excitations):

$$\sum_{j=1}^{N} \int_0^a G(x, x')\sigma_j(x')dx' = \Phi(x) \quad x \in \text{strips} \tag{1}$$

where $G(x, x')$ is the static Green's function, $\Phi(x)$ is the voltage (one or zero on each strip depending on the particular excitation), and $\sigma_j(x')$ is the free charge density on the jth strip.

No general closed form expressions are known for the spatial domain Green's function of our problem, but the spectral domain Green's function (SDGF) can be easily computed (see, for instance, [11], [10]) for an arbitrary layered configuration. According to this, it is more convenient to work with (1) in the spectral domain. A useful technique to solve the spectral domain version of (1) is the Galerkin method. As it has been established in the literature on this subject, Chebyshev polynomials weighed by the Maxwell edge singularity are particularly suitable test and basis functions for the strips free charge density. When these functions are used $\sigma_j(x')$ can be written as follows:

$$\sigma_j(x') = \sum_{q=0}^{q_{\max_j}} a_{q,j}\sigma_{q,j}(x') \tag{2}$$

where

$$\sigma_{q,j}(x') = \begin{cases} \dfrac{2}{\pi w_j}\left[1 - \left(\dfrac{x' - s_j}{w_j/2}\right)^2\right]^{-1/2} \\ \cdot T_q\left(\dfrac{x' - s_j}{w_j/2}\right); x' \in \left[s_j - \dfrac{w_j}{2}, s_j + \dfrac{w_j}{2}\right] \\ 0 \quad \text{elsewhere} \end{cases} \tag{3}$$

The application of the Galerkin method leads to a system of algebraic linear equations for $a_{q,j}$. The entries $A_{p,i}^{q,j}(p = 0, \ldots, p_{\max_i}; q = 0, \ldots, q_{\max_j}; i, j = 1, \ldots, N)$ of this system are the following spectral series:

$$A_{p,i}^{q,j} = \frac{2}{a}\sum_{n=1}^{\infty} \tilde{\sigma}_{p,i}^*(\alpha_n) \cdot \tilde{G}(\alpha_n) \cdot \tilde{\sigma}_{q,j}(\alpha_n) \tag{4}$$

where $\alpha_n = n\pi/a$ is the Fourier variable, $\tilde{G}$ is the SDGF, and $\tilde{\sigma}_{q,j}(\alpha_n)$ are the sine-Fourier transforms of the basis functions in (3):

$$\tilde{\sigma}_{q,j}(\alpha_n) = \begin{cases} J_q\left(\dfrac{\alpha_n w_j}{2}\right)(-1)^{q/2}\sin(\alpha_n s_j) & \text{if } q \text{ is even} \\ J_q\left(\dfrac{\alpha_n w_j}{2}\right)(-1)^{(q-1)/2}\cos(\alpha_n s_j) & \text{if } q \text{ is odd} \end{cases} \tag{5}$$

where J_q is the first kind of Bessel function of order q.

The sum of the series in (4) is the computational step involving meaningful CPU time cost. Therefore, the construction of a highly efficient computer code requires the analytical preprocessing of those series. Kummer's method (extraction of an asymptotic tail) is used in order to accelerate the convergence of the series. According to this method, the series (4) are split as follows:

$$A_{p,i}^{q,j} = \frac{2}{a}\left\{\sum_{n=1}^{\infty} \tilde{\sigma}_{p,i}^*[\tilde{G} - \tilde{G}_{as}]\tilde{\sigma}_{q,j} + S_{p,i}^{q,j}\right\} \tag{6}$$

$$S_{p,i}^{q,j} = \sum_{n=1}^{\infty} \tilde{\sigma}_{p,i}^*\tilde{G}_{as}\tilde{\sigma}_{q,j};$$

$$\tilde{G}_{as} = \frac{1}{2\alpha_n\bar{\epsilon}}$$

$$\bar{\epsilon} = \frac{\epsilon_M + \epsilon_{M+1}}{2} \tag{7}$$

ϵ_k $(k = M, M + 1)$ being the permittivity (or the equivalent permittivity [11], [10] in the anisotropic case) of the kth layer. Since $\tilde{G}_{as}$ is chosen to be the asymptotic behavior of $\tilde{G}$ for large α_n, the remainder series (first term of (6)) converges very quickly. The asymptotic tails $S_{p,i}^{q,j}$ are extremely slow convergent series, but they can be reduced to quasi-analytical expressions by means of the two procedures described in the two following sections.

III. Transformation of the Tails into Power Series

It can be seen from (5) and (7) that the computation of $S_{p,i}^{q,j}$ involves the addition of slowly convergent trigonometrical series of the following kind:

$$(S_{p,i}^{q,j})' = \sum_{n=1}^{\infty} \frac{J_p(nd_i)J_q(nd_j)}{n} \cdot \begin{cases} \cos(nc_{ij}^{\pm}) & \text{if } p + q \text{ even} \\ \sin(nc_{ij}^{\pm}) & \text{if } p + q \text{ odd} \end{cases} \tag{8}$$

where $d_i = \pi w_i/2a$ and $c_{ij}^{\pm} = (\pi/a)(s_j \pm s_i)$.

The residues calculus technique makes it possible to transform (8) into much more quickly convergent power series. The first step is to identify (8) as the addition of the infinite residues

of the following properly chosen complex-plane function:

$$f(z) = \frac{J_p(zd_i)J_q(zd_j)\exp(jzc_{ij}^{\pm})}{z[\exp(j2\pi z) - 1]} \quad p+q \geq 1 \tag{9}$$

When (9) is integrated along the closed path shown in Fig. 2, the residues Cauchy theorem provides an alternative expression for $(S_{p,i}^{q,j})'$:

$$(S_{p,i}^{q,j})' = \left\{ \begin{matrix} (-1)^{(p+q)/2} \\ (-1)^{(p+q-1)/2} \end{matrix} \right\} \int_0^{\infty} dy \frac{I_p(yd_i)I_q(yd_j)}{y\sinh(\pi y)} \cdot \left\{ \begin{matrix} \cosh[(\pi - c_{ij}^{\pm})y]; & p+q \text{ even} \\ \sinh[(\pi - c_{ij}^{\pm})y]; & p+q \text{ odd} \end{matrix} \right. \tag{10}$$

Now, the product of modified Bessel functions I_pI_q is expanded as a series of powers [[16], p. 960] shown in (11) below. F being the hypergeometric function, and Γ being the gamma function. The hypergeometric function $F[-k, -p-k; q+1; (d_j/d_i)^2]$ is a k-degree polynomial in $(d_j/d_i)^2$ shown in (12) below.

In addition, the integrals appearing in (11) are known in closed form. Two alternative expressions [[16], pp. 349–350] for them are:

$$\int_0^{\infty} dy \frac{y^{\mu-1}}{\sinh(\pi y)} \left\{ \begin{matrix} \cosh(\beta y) \\ \sinh(\beta y) \end{matrix} \right\} = \left\{ \begin{matrix} \frac{1}{2}\frac{d^{\mu-1}}{d\beta^{\mu-1}}\tan(\beta/2) \\ \frac{\Gamma(\mu)}{(2\pi)^{\mu}}\left\{\zeta\left[\mu, \frac{1}{2}\left(1-\frac{\beta}{\pi}\right)\right] \pm \zeta\left[\mu, \frac{1}{2}\left(1+\frac{\beta}{\pi}\right)\right]\right\} \end{matrix} \right. \tag{13}$$

where $\mu = p+q+2k, \beta = \pi - c_{ij}^{\pm}$, and ζ is the Riemann's zeta function. The first expression in (13) is used for the first few terms of the k-series. This suffices for most cases, but if larger values of k are needed, the second expression in (13) provides an alternative quick solution.

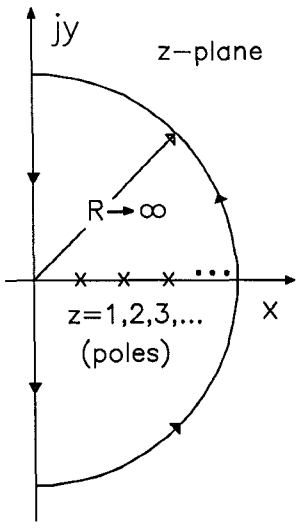

Fig. 2. Integration path in the complex plane for the computation of the spectral series by means of the residues calculus technique.

This procedure is still valid in the case $p+q = 1$ because the new pole of $f(z)$ in $z = 0$ presents a purely imaginary residue. However, the case $p = q = 0$ requires a separate treatment because of the double pole of $f(z)$ in $z = 0$. Let us consider:

$$\frac{d(S_{0,i}^{0,j})'}{dc_{ij}^{\pm}} = -\sum_{n=1}^{\infty} J_0(nd_i)J_0(nd_j)\sin(nc_{ij}^{\pm}) \tag{14}$$

This auxiliary series can be computed by means of the technique explained above when $f(z)$ in (9) is replaced by $g(z) = z \cdot f(z)$. If the power series resulting from this procedure is integrated with respect to $c_{ij}^{\pm}$, expression (15),

$$(S_{p,i}^{q,j})' = \left\{ \begin{matrix} (-1)^{(p+q)/2} \\ (-1)^{(p+q-1)/2} \end{matrix} \right\} \frac{(d_j/d_i)^q}{\Gamma(q+1)} \sum_{k=0}^{\infty} \left(\frac{d_i}{2}\right)^{p+q+2k} \frac{F[-k, -p-k; q+1; (d_j/d_i)^2]}{\Gamma(k+1)\Gamma(p+k+1)} \cdot \int_0^{\infty} dy \frac{y^{p+q+2k-1}}{\sinh(\pi y)} \cdot \left\{ \begin{matrix} \cosh[(\pi - c_{ij}^{\pm})y]; & p+q \text{ even} \\ \sinh[(\pi - c_{ij}^{\pm})y]; & p+q \text{ odd} \end{matrix} \right. \tag{11}$$

$$F[-k, -p-k; q+1; (d_j/d_i)^2] = \sum_{n=0}^{k} \frac{\Gamma(k+1)\Gamma(p+k+1)\Gamma(q+1)(d_j/d_i)^{2n}}{\Gamma(k-n+1)\Gamma(p+k-n+1)\Gamma(q+n+1)\Gamma(n+1)} \tag{12}$$

$$(S_{0,i}^{0,j})' = \sum_{k=1}^{\infty} \frac{\Gamma(2k+1)F[-k, -k; 1; (d_j/d_i)^2]}{2k\Gamma^2(k+1)} \left(\frac{d_i}{4\pi}\right)^{2k} \{\zeta[2k, c_{ij}^{\pm}/2\pi] + \zeta[2k, 1 - c_{ij}^{\pm}/2\pi]\} - \ln[\sin(c_{ij}^{\pm}/2)] + h(d_i, d_j) \tag{15}$$

which is shown at the bottom of this page, is obtained. In this expression, $h(d_i, d_j)$ is the integration constant, which does not need to be calculated because it cancels out when $S_{0,i}^{0,j}$ is computed. It should be noticed that the general expressions presented in this section for the computation of $S_{p,i}^{q,j}$ reduces to the more simple expressions appearing in [15] when the case $i = j$ is considered (basis and testing functions on the same strip).

The power series in this section provide extreme accuracy when just a few terms are retained. In some particular cases (which correspond to rather theoretical than practical situations, such as extremely high coupling levels or very close proximity of the strips to the side walls) more terms need to be considered. Anyway, the Shanks transformation [17, pp. 369–374] provides a useful tool to accelerate the power series in such a way that the technique is even useful in these *critical* cases.

IV. Spatial Domain Computation of the Tails

The second technique considered for the computation of (7) is based on the quasi-analytical integration of the spatial counterpart of the series $S_{p,i}^{q,j}$. By applying Parseval and convolution theorems, we can write (16), which is shown at the bottom of this page, with $G_{as}(x, x')$ being the spatial domain Green's function whose Fourier transform is $\tilde{G}_{as}(\alpha)$, that is:

$$G_{as}(x,x') = \frac{1}{2\pi\epsilon} \ln \left\{ \frac{\sin\left[\frac{\pi}{2a}|x-x'|\right]}{\sin\left[\frac{\pi}{2a}(x+x')\right]} \right\} \tag{17}$$

Note that G_{as} may be physically interpreted as the Green's function of the "asymptotic structure" which results by prolonging the Mth layer to $y = -\infty$ and the $(M+1)$th layer to $y = +\infty$.

The square root in the denominator of the integrands in (16) makes these integrals specially suitable to be computed by means of the Gauss–Chebyshev quadrature formula. However, the direct application of this quadrature to the computation of the convolution integrals is not efficient enough because of the logarithmic singularity of $G_{as}(x, x')$ in $x = x'$. In addition, if the strips #1 and/or #N are very close to the lateral electric walls, $G_{as}(x, x')$ exhibits a quasi-singular behavior when $x + x' \to 0$ or $x + x' \to 2a$. In order to overcome these computational drawbacks, the singular and quasi-singular contributions of $G_{as}(x, x')$ must be extracted out and conveniently treated. The three terms causing the numerical problems can be joined to give the following "singular part" of $G_{as}(x, x')$:

$$S(x,x') = \frac{1}{2\pi\epsilon} \ln \left[\frac{|x-x'|}{(x+x')(2a-x-x')} \right]. \tag{18}$$

It should be noticed that from a physical point of view, $S(x, x')$ accounts for the contributions of the real charge line and the first two image lines reflected by the conducting walls. The convolution integrals shown in (16) at the bottom of the page, can be very efficiently evaluated by splitting the kernel into two parts: $G_{as}(x, x') = S(x, x') + [G_{as}(x, x') - S(x, x')]$. The second term in this expression is a very smooth function. Therefore, its contribution to the convolution is obtained with a low order Chebyshev quadrature. On the other hand, the convolution involving $S(x, x')$ has been analytically evaluated. Let us define $I_{i,j}^{\nu}[q; x]$:

$$I_{i,j}^{\nu}[q;x] = \int_{s_j - w_j/2}^{s_j + w_j/2} dx' \frac{2}{\pi w_j} \frac{T_q\left(\frac{x'-s_j}{w_j/2}\right)}{\sqrt{1-\left(\frac{x'-s_j}{w_j/2}\right)^2}} \cdot \begin{cases} \ln|x-x'| & \text{if } \nu = 0 \\ \ln(x+x') & \text{if } \nu = -1 \\ \ln(2a-x-x') & \text{if } \nu = +1 \end{cases} \tag{19}$$

$$s_i - w_i/2 \le x \le s_i + w_i/2$$

If complex plane integration techniques are used, the closed form expressions shown in (20) at the bottom of this page are obtained for (19), where

$$t_{ij}^{\nu}(x) = \frac{x - s_j^{\nu}}{w_j/2}; \qquad s_i - \frac{w_i}{2} \le x \le s_i + \frac{w_i}{2};$$

$$s_j^{\nu} = \begin{cases} s_j & \text{if } \nu = 0 \\ -s_j & \text{if } \nu = -1 \\ 2a - s_j & \text{if } \nu = +1 \end{cases}$$

$$\frac{2}{a} S_{p,i}^{q,j} = \int_{s_i - w_i/2}^{s_i + w_i/2} dx \frac{2}{\pi w_i} \frac{T_p\left(\frac{x-s_i}{w_i/2}\right)}{\sqrt{1-\left(\frac{x-s_i}{w_i/2}\right)^2}} \int_{s_j - w_j/2}^{s_j + w_j/2} dx' \frac{2}{\pi w_j} \frac{T_q\left(\frac{x'-s_j}{w_j/2}\right)}{\sqrt{1-\left(\frac{x'-s_j}{w_j/2}\right)^2}} G_{as}(x,x') \tag{16}$$

$$I_{i,j}^{\nu}[q;x] = \begin{cases} -\frac{1}{q}\left[t_{ij}^{\nu}(x) - \operatorname{sgn}\left(t_{ij}^{\nu}(x)\right)\sqrt{(t_{ij}^{\nu}(x))^2 - 1}\right]^q (-1)^{(q\cdot\nu)} & \text{if } q \ge 1 \\ \ln\left[\frac{w_j}{4}\left(|t_{ij}^{\nu}(x)| + \sqrt{(t_{ij}^{\nu}(x))^2 - 1}\right)\right] & \text{if } q = 0 \end{cases} \tag{20}$$

and $\mathrm{sgn}(\cdot)$ is the sign function. For the particular case $i = j; \nu = 0$:

$$I^0_{\nu,i}[q;x] = \begin{cases} -\dfrac{1}{q}T_q(t^0_{ii}) & \text{if } q \geq 1 \\ \ln(w_i/4) & \text{if } q = 0 \end{cases} \tag{21}$$

The next step for the computation of (16) is to carry out the inner products. Only the part involving $I^0_{i,i}$ has been found to have a closed form:

$$\int_{s_i - w_i/2}^{s_i + w_i/2} dx \frac{2}{\pi w_i} \frac{T_p\left(\dfrac{x - s_i}{w_i/2}\right)}{\sqrt{1 - \left(\dfrac{x - s_i}{w_i/2}\right)^2}} I^0_{i,i}[q;x]$$

$$= \begin{cases} -1/2p & \text{if } p = q \neq 0 \\ 0 & \text{if } p \neq q \\ \ln(w_i/4) & \text{if } p = q = 0 \end{cases} \tag{22}$$

The rest of the inner products have been numerically evaluated by low order Gauss-Chebyshev quadratures.

In most cases, the number of points employed in both convolution and inner product quadratures has been two or three more than the number of basis functions used on each strip. This is sufficient to ensure more than eight significant figures in the calculations. Nevertheless, the computer program which implements this technique makes it possible to introduce a larger number of quadrature points for the inner product integrals involving $I^{-1}_{1,1}, I^{+1}_{N,N}$, and $I^0_{i,i+1}$ $(i = 1, \cdots, N-1)$. This possibility can be useful because these inner products require a few more quadrature points in the *critical* cases mentioned at the end of Section III (if similar accuracy is required for all the inner products).

V. Numerical Results

Two double precision FORTRAN codes have been written to implement the techniques discussed above. Exhaustive numerical work has been carried out to validate the computer codes on both a PC/386 computer (with math coprocessor) and a VAX/6410. This work has been useful to establish the parameters which have an influence on the accuracy and efficiency of the two alternative methods proposed in this paper.

Firstly, we have checked the convergence of the series (11) and (15). The convergence of $(S^{q,j}_{p,i})'$ has been found to be mainly affected by the ratios $r^+_{ij} = w_i + w_j/2(s_j + s_i)$ and $r^-_{ij} = w_i + w_j/2(s_j - s_i)$. In most practical situations, the convergence is reached in few terms. Nevertheless, the convergence becomes slower when r^+_{ij} and/or r^-_{ij} are very close to one (unity). This occurs if some strip is very close to the lateral metallic walls $(r^+_{ij} \approx 1)$ and/or if very tightly coupled strips are present $(r^-_{ij} \approx 1)$. In these cases, more terms must be retained to add up the corresponding series. In Table I we show a typical convergence pattern for the series $S^{0,j}_{0,i}$ associated to a pair of asymmetrical strips for different coupling levels. The number of terms required in the computation of $S^{0,2}_{0,1}$ increases when r^-_{12} approaches to unit. For this study five significant correct figures are always imposed in the computation of $C_{1,1}$.

TABLE I
Maximum Number of Terms $k_{\max}$ of the Series $S^{0,j}_{0,i}$ $i,j = 1,2$ to be Retained for Five Significant Figures Accuracy in the Capacitance. The Asterisked Column Includes the Results Obtained by Using the Twice Iterated Shanks Transformation (Data $a = 10., h_1 = 1., h_2 = 2., w_1 = 1., w_2 = 2., s_1 = 3.$).

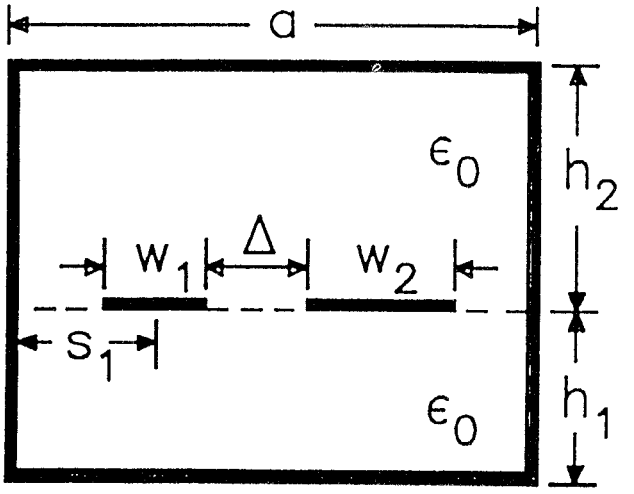

Δ	r^-_{12}	k_{max}			
		$S^{0,1}_{0,1}$	$S^{0,2}_{0,2}$	$S^{0,2}_{0,1}$	$(S^{0,2}_{0,1})^*$
2.00	0.43	0	0	1	-
1.00	0.60	1	1	4	3
0.50	0.75	1	2	8	5
0.10	0.94	2	2	35	16
0.05	0.97	3	3	79	36
0.01	0.99	3	3	229	94

Note that the use of the twice iterated Shanks transformation (asterisked column) introduces a significant acceleration (over 50%) in the convergence of this series. It must be emphasized that the cases involving a very large $k_{\max}$ are not realistic. Anyway, the direct summation of the original Fourier series would require much more computational effort (prohibitive if very high accuracy is desired). Therefore the application of this technique is always preferable to direct summation.

The spatial domain technique presents similar difficulties in the same cases, but it has been found to be less sensitive to those problems. In general, the convolution integral and the inner products are very accurately computed by using a number of quadrature points equal to or slightly larger than the number of basis functions employed on each strip. Typical computations are so accurate that more than eight meaningful digits can be obtained for the coefficients of the expansion of the charge distribution. However, when r^+_{ij} and/or r^-_{ij} take (theoretical rather than practical) values very close to 1, the number of quadrature points N^*_q used for the computation of the critical inner products involving $I^{-1}_{1,1}, I^{+1}_{N,N}$ and/or $I^0_{i,i+1}$ $(i = 1, \ldots, N-1)$ must be increased to keep the accuracy pattern. In Table II, we display the values of N^*_q needed to get both five and ten significant figures

TABLE II
NUMBER OF GAUSS– CHEBYSHEV QUADRATURE POINTS N_q^* USED IN THE CRITICAL INNER PRODUCT INVOLVING $I_{1,2}^0$ TO GET BOTH FIVE AND TEN SIGNIFICANT FIGURES CAPACITANCES. (DATA: EQUAL TO THOSE IN TABLE I).

Δ	r_{12}^-	N_q^* (5 digits)	N_q^* (10 digits)
2.00	0.43	2	4
1.00	0.60	2	5
0.50	0.75	3	7
0.10	0.94	5	13
0.05	0.97	7	20
0.01	0.99	11	35

of $C_{1,1}$ for different coupling levels. In that example, the convolution integrals and the non-critical inner products have been computed with 4 Gauss–Chebyshev quadrature points.

The aspects discussed in the previous paragraphs deal with the quality of the computations of the Galerkin matrix entries. However, the accuracy of the capacitance and inductance coefficients also depends on the number of basis functions. The trial functions in (3) are very suitable for the multistrip problem, since extreme accuracy for both capacitance coefficients and charge distribution can be achieved in all practical situations. Typical results obtained with our programs (both programs provide exactly the same results within the computer accuracy) can be seen in Tables III and IV. From Table III, it can be seen that more trial functions are required when the strips are very close or when they are adjacent to thin dielectric layers (the strips are in this case relatively wide in comparison with the thicknesses of the layers). Anyway, from a practical point of view, no more than three or four basis functions are necessary to obtain useful highly accurate results. Table IV shows an example of the expansion coefficients obtained for the charge distribution when different number of basis functions are used. The coefficients of the expansion are not sensitive to the addition of new terms when convergence has been achieved (this fact suggests that (2, 3) is a quasi-orthogonal expansion). As it is expected from the stationary nature of the first coefficient, this is much more accurately computed than the charge distribution.

In our opinion, an important feature of the methods reported in this paper is that when they are used, no numerical problems arise if the number of basis functions is increased. In the past, the authors have used other asymptotic tails—involving large argument approximation of the Bessel functions—to accelerate the convergence of the spectral series [18]. For most practical purposes, that approach works properly (although more slowly than those presented in the present paper), but some problems can be observed when a relatively large number of basis functions are used. This is a consequence of cumulative numerical errors when series involving large order Bessel functions need to be computed. This drawback has not been detected with the methods developed in the present work.

The numerical data generated with our programs have been compared with highly accurate data (or exact solutions) reported in the literature for particular structures. The agreement has been always found to be excellent (all the significant figures reported have been invariably obtained). For example, numerical data for the capacitance coefficients of a five strips striplike configuration in homogeneous medium are reported in [[8], Table VII] and [[7], Fig. 6]. The former uses an enhanced integral equation technique and extrapolation procedures and the latter gives a conformal mapping solution (although numerical computation of the hiperelliptic functions is required). Five figures are correctly given in [8] and six figures are given in [7] for the normalized capacitance coefficients. Our programs reproduce all the significant figures reported in those works. To obtain five figures accuracy, 4 basis functions have been retained on each strip, and the CPU time was about 1.5 seconds on a PC/386 computer (about 0.15 seconds on a VAX/6410). Six figures were obtained with 5 basis functions (2.2 seconds on a PC/386 computer, about 0.2 seconds on a VAX/6410). These CPU times refer to the spatial domain technique. The same results were obtained by means of the other technique described in this paper with slightly higher CPU times. As a final example, in Table V we compare our results with

TABLE III
CONVERGENCE OF THE CAPACITANCE MATRIX (NORMALIZED TO ϵ_0) VERSUS THE NUMBER OF BASIS FUNCTIONS ($p_{\max}$) DATA: $\epsilon_{rr2} = 13, \epsilon_{yy2} = 10, \epsilon_{rr3} = \epsilon_{yy3} = 2.54, a = 20$ mm, $s_1 = 9.45$ mm, $w_1 = 1$ mm, $w_2 = 1.5$ mm, CASE I ($h_1 = 0, h_2 = 0.635$ mm, $h_3 = 0, h_4 = 10$ mm), CASE II ($h_1 = 0.51$ mm, $h_2 = 0.125$ mm, $h_3 = 0.125$ mm, $h_4 = 9.875$ mm).

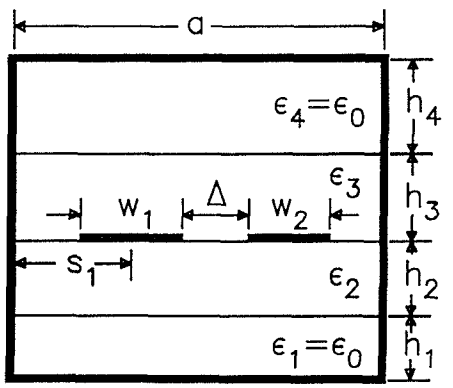

Cases	p_{max}	$\Delta = 0.1mm$			$\Delta = 1mm$		
		C_{11}	C_{12}	C_{22}	C_{11}	C_{12}	C_{22}
I	1	28.7199	-7.73533	37.1587	27.1524	-1.22612	35.1310
	2	30.8053	-9.00472	39.1877	27.1841	-1.22926	35.1583
	3	31.3147	-9.04270	39.4832	27.2127	-1.19820	35.2954
	4	31.4238	-9.11756	39.5505	27.2132	-1.19824	35.2955
	5	31.4439	-9.13304	39.5639	27.2132	-1.19829	35.2956
	6	31.4479	-9.13600	39.5663	27.2132	-1.19829	35.2956
	7	31.4488	-9.13669	39.5663	-	-	-
	8	31.4490	-9.13687	39.5671	-	-	-
	9	31.4491	-9 13692	39.5671	-	-	-
	10	31.4491	-9.13694	39 5671	-	-	-
	11	31.4491	-9.13694	39.5671	-	-	-
II	1	8.70529	-4.73082	10.1254	6.87581	-1 74542	7.99884
	2	11 9197	-7 53461	13.0869	7.06826	-1.83526	8.14886
	3	13.5927	-9.20794	14.7678	7.18892	-1.94238	8.28897
	4	13.9190	-9.49782	15.0354	7.19602	-1.94558	8.29218
	5	13.9838	-9.56780	15.1115	7.19838	-1.94896	8.29925
	6	13.9914	-9.57426	15.1170	7.19849	-1.94900	8.29927
	7	13.9920	-9.57489	15.1177	7 19850	-1.94901	8.29928
	8	13.9920	-9.57491	15.1177	7.19850	-1.94901	8.29928
	9	13.9920	-9 57491	15.1177	-	-	-

TABLE IV
CHARGE DISTRIBUTION COEFFICIENTS OF A PAIR OF ASYMMETRICAL COUPLED STRIPS FOR DIFFERENT VALUES OF THE NUMBER OF BASIS FUNCTIONS q_{max}. DATA: EQUAL TO THOSE IN TABLE III, CASE I, $\Delta = 1$ mm.

		Excit. (1,0)		Excit. (0,1)	
q_{max}	q	$a_{q,1}$	$a_{q,2}$	$a_{q,1}$	$a_{q,2}$
1	1	27.1524	-1.22612	-1.22612	35.1310
2	1	27.1841	-1.22926	-1.22926	35.1583
	2	0.09538	1.70030	-1.51918	-0.11748
3	1	27.2127	-1.19820	-1.19820	35.2954
	2	0.10092	1.68933	-1.48469	-0.11830
	3	-1.95733	-0.82322	-0.55950	-4.65142
4	1	27.2132	-1.19824	-1.19824	35.2955
	2	0.10152	1.68674	-1.48439	-0.11827
	3	-1.95706	-0.82325	-0.55952	-4.65132
	4	0.01094	0.31610	-0.15337	-0.02298
5	1	27.2132	-1.19829	-1.19829	35.2956
	2	0.10156	1.68675	-1.48446	-0.11828
	3	-1.95705	-0.82309	-0.55955	-4.65161
	4	0.01094	0.31610	-0.15338	-0.02298
	5	0.04654	-0.09211	-0.03038	0.16107
6	1	27.2132	-1.19829	-1.19829	35.2956
	2	0.10156	1.68676	-1.48446	-0.11829
	3	-1.95705	-0.82309	-0.55955	-4.65161
	4	0.01094	0.31609	-0.15338	-0.02298
	5	0.04654	-0.09211	-0.03038	0.16107
	6	0.00033	0.02020	-0.00439	-0.00150

those obtained by the method of lines (with nonequidistant discretization) in [5] for a five conductor microstrip structure with different widths and inhomogeneous substrate. To obtain 4 digits accuracy we have used 5 basis functions, and the CPU time was less than 1.5 seconds (PC/386). A fraction of a second was necessary to get the same level of accuracy of the example in [5]. In general, very reliable and accurate results can be obtained for the capacitance and inductance matrices of microstrip structures on a PC/386 computer with CPU times ranging from a fraction of a second to two or three seconds (depending on the number of strips and basis functions). The surface charge distributions are also provided with very good accuracy.

VI. CONCLUSIONS

In the present work, a numerically improved spectral domain approach is employed for the efficient and accurate quasi-TEM analysis of a wide class of multistrip transmission lines. A proper analytical preprocessing is incorporated in the computation of the entries of the Galerkin equations system in order to achieve extreme accuracy in a short CPU time. To reach this goal, two different techniques have been proposed and compared. The double precision FORTRAN programs implementing these techniques are able to analyze multistrip configurations embedded in multilayered substrates on a PC/386 computer in less than a few seconds. Total agreement has been found with exact results (up to the accuracy reported in the literature) for simple particular configurations. Good agreement has been also found with many other results reported for more general structures. The surface charge distribution can be obtained with accuracy and reliability if this quantity is required.

TABLE V
COMPARISON BETWEEN OUR RESULTS AND THOSE REPORTED IN [5] FOR THE CAPACITANCE MATRIX (NORMALIZED TO ϵ_0) OF A FIVE-CONDUCTOR MICROSTRIP CONFIGURATION. DATA: $h = 0.8$ mm, $\epsilon = 2.5\epsilon_0$, $w_1 = 0.16$ mm, $w_2 = 0.47$ mm $\Delta = 0.07$ mm, $a = 3.7$ mm.

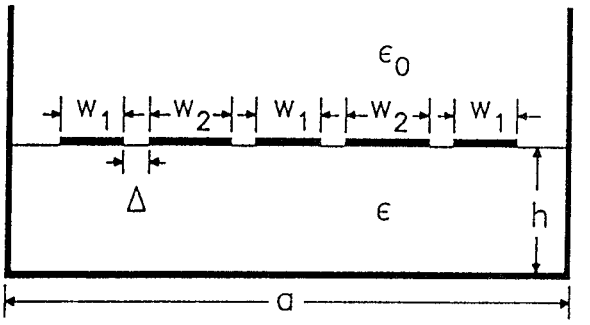

C_{ij}/ϵ_0	Diestel [5]	This work
$C_{11}/\epsilon_0 = C_{55}/\epsilon_0$	4.633	4.642
$C_{22}/\epsilon_0 = C_{44}/\epsilon_0$	7.857	7.871
C_{33}/ϵ_0	5.723	5.738
$C_{12}/\epsilon_0 = C_{45}/\epsilon_0$	-2.547	-2.555
$C_{23}/\epsilon_0 = C_{34}/\epsilon_0$	-2.338	-2.346
$C_{13}/\epsilon_0 = C_{35}/\epsilon_0$	-0.080	-0.080
C_{24}/ϵ_0	-0.553	-0.553
$C_{14}/\epsilon_0 = C_{25}/\epsilon_0$	-0.064	-0.064
C_{15}/ϵ_0	-0.013	-0.013

REFERENCES

[1] C. Wei, R. F. Harrington, J. R. Mautz, T. K. Sarkar, "Multiconductor transmission lines in multilayered dielectric media," *IEEE Trans. Microwave Theory Tech.*, vol. MTT-32, pp. 439–450, Apr. 1984.
[2] Z. Pantic and R. Mittra, "Quasi-TEM analysis of microwave transmission lines by the finite-element method," *IEEE Trans Microwave Theory Tech.*, vol. MTT-34, pp. 1096–1103, Nov. 1986.
[3] F. Olyslager, N. Faché, and D. de Zutter, "New fast and accurate line parameter calculation of general multiconductor transmission lines in multilayered media," *IEEE Trans. Microwave Theory Tech.*, vol. 39, pp. 901–909, June 1991.
[4] V. K. Tripathi and R. J. Bucolo, "A simple network analog approach for the quasi-static characteristics of general lossy, anisotropic, layered structures," *IEEE Trans Microwave Theory Tech*, vol. MTT-33, pp. 1458–1464, Dec. 1985.
[5] H. Diestel, "Analysis of planar multiconductor transmission-line systems with the method of lines," *AEU*, vol. 41, pp. 169–175, 1987.
[6] L. J. P. Linner, "A method for the computation of the characteristic immitance matrix of multiconductor striplines with arbitrary widths," *IEEE Trans. Microwave Theory Tech.*, vol. MTT-22, pp. 930–937, Nov. 1974.
[7] D. Homentcovschi, A. Manolescu, A. M. Manolescu, and L. Kreindler, "An analytical solution for the coupled stripline-like microstrip line problem," *IEEE Trans Microwave Theory Tech*, vol. MTT-36, pp. 1002–1007, June 1988.
[8] D. W. Kammler, "Calculation of characteristic admittances and coupling coefficients for strip transmission lines," *IEEE Trans Microwave Theory and Tech.*, vol. MTT-16, pp. 925–937, Nov. 1968.

[9] T. Kitazawa and Y. Hayashi, "Asymmetrical three-line coupled striplines with anisotropic substrates," *IEEE Trans. Microwave Theory Tech.*, vol. MTT-34, pp. 767–772, July 1986.
[10] M. Horno, F. L. Mesa, F. Medina, and R. Marqués, "Quasi-TEM analysis of multilayered, multiconductor coplanar structures with dielectric and magnetic anisotropy including substrate losses," *IEEE Trans. Microwave Theory Tech.*, vol. 38, pp. 1059–1068, Aug. 1990.
[11] F. Medina and M. Horno, "Upper and lower bounds on mode capacitances for a large class of anisotropic multilayered microstrip-like transmission lines," *Proc. Inst. Elec. Eng. (Microwaves, Optics & Antennas)*, vol. 132, no. 3, pp. 157–163, June 1985.
[12] A. Sawicki and K. Sachse, "Lower and upper bound calculations on the capacitance of multiconductor printed transmission line using the spectral-domain approach and variational method," *IEEE Trans. Microwave Theory Tech.*, vol. MTT-34, pp. 236–244, Feb. 1986.
[13] C. H. Chan and R. Mittra, "Analysis of MMIC structures using an efficient iterative approach," *IEEE Trans. Microwave Theory Tech.*, vol. 36, pp. 96–105, January 1988.
[14] E. Drake, F. Medina, and M. Horno, "An improved iterative technique for the quasi-TEM analysis of generalized planar lines," *IEEE Trans. Microwave Theory Tech.*, vol. 40, Apr. 1992.
[15] F. Medina and M. Horno, "Quasi-analytical static solution of the boxed microstrip line embedded in a layered medium," *IEEE Trans. Microwave Theory Tech.*, vol. 40, Sept. 1992.
[16] I. S. Gradshteyn and I. M. Rythik, *Table of Integrals, Series and Products*. New York: Academic Press, 1980.
[17] C. M. Bender and S. A. Orszag, *Advanced Mathematical Methods for Scientists and Engineers*. New York: McGraw-Hill, 1978.
[18] F. Medina and M. Horno, "Spectral and variational analysis of generalized cylindrical and elliptical strip and microstrip lines," *IEEE Trans. Microwave Theory Tech.*, vol. 38, pp. 1287–1293, Sept. 1990.

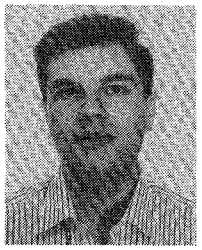

Enrique Drake was born in Montilla, Córdoba, Spain, on September 4, 1966. He received the Licenciado degree in physics from the University of Seville, Spain, in 1990. He is currently following a Ph.D. program in Microwaves with a scholarship of the Spanish Government. His research interest focus on the analysis of planar structures and multiconductor lines.

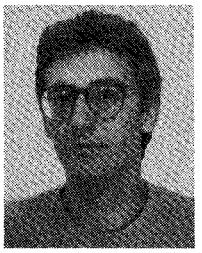

Francisco Medina (M'91) was born in Puerto Real, Cádiz, Spain, on November, 1960. He received the Licenciado degree in September 1983 and the Doctor degree in 1987, both in physics, from the University of Seville, Spain.

He is currently Associate Professor of Electricity and Magnetism in the Department of Electronics and Electromagnetics, University of Seville. His research deals mainly with analytical and numerical methods for planar structures and multiconductor lines.

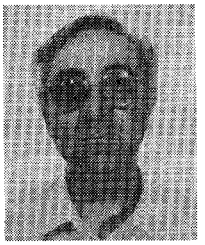

Manuel Horno (M'75) was born in Torre del Campo, Jaén, Spain. He received the Licenciado degree in Physics in June 1969, and the Doctor degree in physics in January 1972, both from the University of Seville, Spain.

Since October 1969 he has been with the Department of Electronics and Electromagnetism at the University of Seville, where he became an Assistant Professor in 1970, Associate Professor in 1975 and Professor in 1986. He is a member of the Electromagnetism Academy of M.I.T., Cambridge. His main fields of interest include boundary value problems in electromagnetic theory, wave propagation through anisotropic media, and microwave integrated circuits. He is presently engaged in the analysis of planar transmission lines embedded in anisotropic materials, multiconductor transmission lines, and planar slow-wave structures.